Chemosphere 270 (2021) 129491

Contents lists available at ScienceDirect

Chemosphere

journal homepage: www.elsevier.com/locate/chemosphere

Treatment of two sartan antihypertensives in water by photo-electro-Fenton using BDD anodes: Degradation kinetics, theoretical analyses, primary transformations and matrix effects

Diana Martínez-Pachón [a], Efraím A. Serna-Galvis [b, c], María Ibañez [d], Félix Hernández [d], Yenny Ávila-Torres [e], Ricardo A. Torres-Palma [b, *], Alejandro Moncayo-Lasso [a, **]

[a] Grupo de Investigación en Ciencias Biológicas y Químicas, Facultad de Ciencias, Universidad Antonio Nariño (UAN), Bogotá D.C., Colombia
[b] Grupo de Investigación en Remediación Ambiental y Biocatálisis (GIRAB), Instituto de Química, Facultad de Ciencias Exactas y Naturales, Universidad de Antioquia UdeA, Calle 70 No. 52-21, Medellín, Colombia
[c] Grupo de Investigaciones Biomédicas Uniremington, Facultad de Ciencias de La Salud, Corporación Universitaria Remington (Uniremington), Calle 51 No. 51-27, Medellín, Colombia
[d] Research Institute for Pesticides and Water (IUPA), University Jaume I (UJI), Castellón, Spain
[e] Grupo de Investigación QUIBIO, Facultad de Ciencias Básicas, Universidad Santiago de Cali, Santiago de Cali, Pampalinda, Colombia

HIGHLIGHTS

- Sartan-antihypertensives degraded by photo-electro-Fenton (PEF) at mild current, light, and iron concentration.
- The structural differences between LOS and VAL determined their interaction with the degrading agents.
- LOS exhibited a higher reactivity than VAL toward the electrogenerated species.
- Partial mineralization of target pollutants indicates that byproducts are more recalcitrant to action of PEF.
- The PEF process led to a high degradation of LOS in actual effluents despite interfering effects of matrix components.

GRAPHICAL ABSTRACT

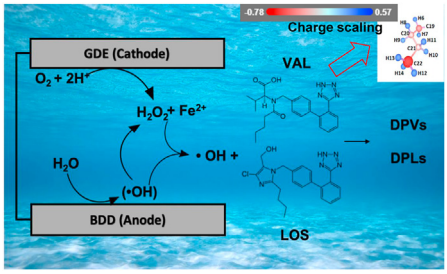

ARTICLE INFO

Article history:
Received 4 August 2020
Received in revised form
23 December 2020
Accepted 26 December 2020
Available online 30 December 2020

Handling Editor: Derek Muir

ABSTRACT

Degradation of two representative antihypertensives, losartan (LOS) and valsartan (VAL) in water by photo-electro-Fenton (PEF), using a BDD anode in presence of sulfate anion was evaluated. PEF showed a fast elimination of these pollutants (>95% at 30 and 60 min of treatment for LOS and VAL, respectively). The main elimination route was the attacks of radicals produced in the system, having pseudo-first-order rate constants of 0.154 and 0.054 min^{-1} for LOS and VAL, correspondingly. Theoretical analyses of atomic charges were performed to rationalize the antihypertensives reactivity toward the electrogenerated degrading agents. Afterwards, the primary transformation products were assessed. The transformation products revealed that the degrading species attack the biphenyl-tetrazole, imidazole, and alcohol moieties on LOS. Meanwhile, carboxylic and amide groups, plus the central nucleus, were modified on

* Corresponding author.
** Corresponding author.
E-mail addresses: ricardo.torres@udea.edu.co (R.A. Torres-Palma), amoncayo@uan.edu.co (A. Moncayo-Lasso).

https://doi.org/10.1016/j.chemosphere.2020.129491

Keywords:
Advanced oxidation process
Electrochemical techniques
Losartan
Pollutant elimination
Valsartan
Water treatment

VAL. These moieties corresponded well with the electron-rich sites indicated by the theoretical calculations. Also, the PEF process removed between 33 and 38% of total organic carbon after 5 h of electrolysis. Finally, it was considered LOS treatment in presence of oxalic acid (a typical organic waste of pharmaceutical industry), in addition to the pollutant degradation in effluents from municipal sewage treatment plants by PEF at pH ~5. Oxalic acid accelerated LOS degradation. Meanwhile, in the effluent, the process led to 64% of LOS removal after 120 min of treatment, indicating the high potentiality of PEF to degrade antihypertensives in water containing organic and inorganic substances.

1. Introduction

Sartan-type antihypertensives are highly prescribed pharmaceuticals, which, after consumption, are partially metabolized, and thus significant amounts are excreted into the sewage system (Israili, 2000). Indeed, the sartan-type antihypertensives are frequently found in influents of municipal wastewater treatment plants (Botero-Coy et al., 2018; Gurke et al., 2015; Kaur and Dulova, 2020). Furthermore, the conventional processes (as secondary biological systems) cannot completely degrade sartan-type antihypertensives. Consequently, unmodified or partially modified antihypertensives are released into the environment through municipal wastewater treatment plants (Botero-Coy et al., 2018; Gurke et al., 2015; Kaur and Dulova, 2020). It must be mentioned that LOS and VAL are among the most prescribed/consumed antihypertensives worldwide. For instance, ~52 and ~9 million of losartan and valsartan prescriptions were done in the USA during 2017 (ClinClac, 2018; Mikulic, 2020).

LOS and VAL have been detected in diverse water bodies. Specifically, these antihypertensives have been found in water sample from beaches (LOS: 3.6−548.0 ng/L) (Roveri et al., 2020), influents (LOS: 2.18 μg/L, VAL: 1.62 μg/L) and effluents (LOS: 1.97 μg/L, VAL: 1.05 μg/L) of municipal wastewater treatment plants (Botero-Coy et al., 2018), hospital wastewaters (VAL:17.7 μg/L) (Serna-Galvis et al., 2019a), and rivers (VAL: 0.11−1.10 μg/L) (Bayer et al., 2014). Additionally, it is reported that in the environment, sartan-type antihypertensives as LOS or VAL are transformed into valsartan-acid, which is a persistent substance (Berkner and Thierbach, 2014; Nödler et al., 2013). Also, some researches have shown that LOS could raise moderate to severe risks to aquatic organisms such as algae, crustaceans and fishes (Roveri et al., 2020), and induce chronic effects on *Lemna minor* growth (Godoy et al., 2015). Hence, processes to efficiently degrade sartan-type pollutants in aqueous matrices and limit their input to natural media are required.

Among processes that have shown high efficiency for degrading toxic and/or recalcitrant pollutants are electrochemical treatments (Dao et al., 2020; Moreira et al., 2017). Particularly, the electrochemical treatments involving the utilization of hydroxyl radical ($HO^{\bullet}$, E°: 2.8 V) possess a high ability to transform the organic pollutants into innocuous substances (even up to mineralization) (Feng et al., 2019; Moreira et al., 2017). Electrochemical processes have high cost-effectiveness in electric energy consumption, versatility, and environmental compatibility (Salazar et al., 2016).

In this work is studied the electrochemical treatment, mainly PEF using BDD anodes, of LOS and VAL. Degradation under mild electrochemical conditions (low current density, low UVA power, and small iron concentration) was tested. Although previous researches have tested the degradation of LOS using electro-oxidation (Salazar et al., 2016), such work does not present the pollutant's treatment in complex water matrices as effluents of municipal wastewater treatment plants.

Also, it must be mentioned that LOS and VAL eliminations by PEF using DSA anodes and sodium chloride as supporting electrolytes have been informed (Martínez-Pachón et al., 2018, 2019). However, this configuration involves active chlorine action, which may lead to the formation of organ-chlorinated compounds. Moreover, under the authors' knowledge, the utilization of theoretical calculations (to study the antihypertensives reactivity) has not been reported. Thus, herein, it was considered the treatment of both antihypertensives by electrochemical processes based on BDD as anode and sodium sulfate as supporting electrolyte (to promote the action of radicals more than chlorine species). Furthermore, atomic charge analyses were performed to study the pollutants reactivity toward oxidizing agents generated in the electrochemical processes.

Therefore, our work develops four main topics: 1) Evaluation of the efficiency of the photo-electro-Fenton (PEF) processes to degrade LOS and VAL individually, in addition to the determination of process action routes (using control experiments, cyclic voltammetry and quantification of oxidants); 2) Testing of the antihypertensive structure effect on the elimination by PEF, comparing the elimination of losartan and valsartan, and performing theoretical analyses of atomic charge to provide a basic idea about the reactivity of the antihypertensives toward oxidizing agents; 3) Determination of primary transformation products (by using HPLC-MS technique) and mineralization of both antihypertensives by PEF action; 4) Assessment of matrix effects through degradation of the LOS in effluents of municipal wastewater treatment plant by PEF at a pH higher than 3.0, in addition to the treatment in the presence of a typical organic waste of pharmaceutical industry.

2. Materials and methods

2.1. Reagents

Valsartan and losartan potassium (99% purity) were purchased from Sigma Aldrich. Iron (II) sulfate heptahydrate ($FeSO_4 \cdot 7H_2O$), potassium phosphate dibasic (K_2HPO_4), orthophosphoric acid (H_3PO_4), potassium hydrogen phthalate ($C_8H_5KO_4$), oxalic acid ($C_2H_2O_4$) and sodium sulfate (Na_2SO_4) were analytical grade from Merck. The pH of the solutions was adjusted using chlorhydric acid (HCl, 98% purity). Methanol (MeOH) and acetonitrile (CH_3CN) HPLC-grade were obtained from Panreac. All solutions were prepared with ultrapure water produced by a Millipore Milli-Q system with resistivity >18 MΩ cm at 25 °C, and the experiments were carried out at least by duplicate. For UHPLC-HRMS analysis, HPLC-grade water was obtained by purifying demineralized water using a Milli-Q system from Millipore (Bedford, MA, USA). HPLC-grade methanol and acetonitrile, formic acid, acetone, and sodium hydroxide were acquired from Scharlau. Leucine enkephalin was purchased from Sigma-Aldrich (St. Louis, MO, USA).

2.2. Reaction systems

The degradation experiments were carried out in an open undivided 250-mL electrolytic cell (Fig. SM1), operated in batch mode at room temperature. For the photo-electro-Fenton process, a carbon-felt air diffusion cathode (GDE, 2 cm^2) and a boron-doped diamond anode (BDD, 2.0 cm^2, which was supplied by Adamant Technologies (Neuchatel, Switzerland) and synthesized by the hot filament chemical vapor deposition technique) were used. Ferrous ions (36 μmol/L) were added to the solution, and it was irradiated with a UVA light lamp (fluorescent black-light blue tube Toshiba FL4BLB/4 W, wavelength 368 nm, photoionization energy input of 1.4 W/m^2) placed inside the cell. The electrodes were located in the center of the reactor at 2.0 cm of distance.

The experimental conditions (current density, supporting electrolyte concentration, iron concentration, pollutants amount, reaction volume, reactor configuration, etc.) were chosen considering previous works of our research team (Martínez-Pachón et al., 2018, 2019), and similar researches from the literature (Olvera-Vargas et al., 2021). All experiments were carried at 5 mA/cm^2 of current density. The electrochemical cell, containing LOS or VAL that were individually treated (200 mL, at 45 μmol/L each), was bubbled with air obtained from an air compressor to saturate the solution with oxygen; and continuous stirring (400 rpm on a magnetic stirrer ARECT by VELP Scientifica) was provided. Sodium sulfate (0.05 mol/L) was used as supporting electrolyte, and when necessary, the initial pH-value was adjusted at 3.0 with hydrochloric acid solution (0.1 mol/L). For control experiments as anodic oxidation (AO), the electrode arrangement was boron-doped diamond anode (BDD)/stainless steel cathode (SS, 2 cm^2).

Some experiments were carried out to evaluate the LOS degradation by PEF at higher pH values and in aqueous matrices more complex than distilled water. In such case, the PEF process was carried out in the presence of oxalic acid (40 μmol/L) without pH modification and doping with LOS the effluent of the wastewater treatment plant Salitre-Bogotá-Colombia (EWWTP).

2.3. Analyses

The antihypertensives degradation was followed using an HPLC Shimadzu LC-20AT equipped with a photodiode array detector SPD-M20A and a C18 column (Waters Spherisil ODS 2, 250 mm × 4.6 mm i.d., 5 μm particle size). The mobile phase was composed of phosphate buffer (pH 3.5, 0.01 mol/L)/acetonitrile/methanol (44/46/10 v/v/v) at 25 °C, using isocratic conditions). The mixture was pumped at 1.0 mL/min flow rate, and the detector was set up at 254 nm. Under these conditions, LOS and VAL were eluted at 3.5 min and 6.9 min, respectively.

Cyclic voltammetry (CV) analyses were performed in a ZAHNER IM6 potentiostat-galvanostat using Na_2SO_4 at 0.05 mol/L as supporting electrolyte in a conventional three-electrode cell. BDD anode was used as the working electrode, Ag/AgCl (3.0 M KCl) as the reference electrode and the stainless-steel cathode (SS) as the counter electrode. The CV measurement was conducted at a sweep rate of 20 mV s^{-1}.

Transformation products were elucidated by UHPLC-HRMS, using a Waters Acquity UHPLC system (Waters, Milford, MA, USA), coupled to a hybrid quadrupole-orthogonal acceleration-time of flight mass spectrometer (XEVO G2 QTOF, Waters Micromass, Manchester, UK), with an orthogonal Z-spray-ESI interface, operated in both positive and negative ionization modes. Additional details on instrumental conditions can be seen elsewhere (Martínez-Pachón et al., 2019; Serna-Galvis et al., 2019b).

For MS^E experiments, two functions were acquired: for the low energy function (LE) collision energy of 4 eV was selected whereas for the high energy (HE) function, a collision energy ramp from 15 to 40 eV was applied, in order to obtain a greater range of fragment ions. Additional MS/MS experiments at different collision energies (10, 20, 30, 40 and 50 eV) were also performed. Mass data was acquired with a MassLynx v 4.1 (Waters).

Accumulation of hydrogen peroxide electrogenerated was estimated by iodometry (Serna-Galvis et al., 2015). An aliquot of 30 μL from the reactor was added to a quartz cell containing 1920 μL of potassium iodide (0.1 mol/L) and 50 μL of ammonium heptamolybdate (0.01 mol/L). The sample was homogenized using a vortex mixer, and after 5 min, the absorbance at 350 nm was measured using a Mettler Toledo UV5 spectrophotometer.

The mineralization of LOS and VAL treated solutions were monitored by the abatement of total organic carbon (TOC), which was measured using a Shimadzu LCSH TOC analyzer. The TOC was determined by combustion with catalytic oxidation at 680 °C using high-purity oxygen as the carrying gas at a flow rate of 190 mL/min with a non-dispersive infrared detector. The calibration of the analyzer was attained with standard potassium hydrogen phthalate (99.5%) solution.

Theoretical analyses of atomic charge (AC, which provides a basic idea on the electron density (Ionescu et al., 2015)) for losartan and valsartan were performed by using the free online AtomicChargeCalculator© (version 1.0.17.1.26) software by loading the structure of the molecules in PDB or SDF format (Sehnal, 2020).

3. Results and discussion

3.1. Action routes of the photo-electro-Fenton in the treatment of the antihypertensives

Initially, the degrading ability of the photo-electro-Fenton (PEF) system on the antihypertensives was tested. Fig. 1 presents the evolution of both pollutants under the PEF process. It can be noted that at 30 min of electrolysis, PEF achieved ~80 and 100% of the VAL and LOS removals, respectively. This process may involve the action of hydroxyl radical physisorbed on the BDD anode and the persulfate electrogenerated from the supporting electrolyte (i.e., the mediated routes, Eqs. (1)–(3)), in addition to direct oxidation by electron transfer from the pharmaceuticals to the anode (Eq. (4))

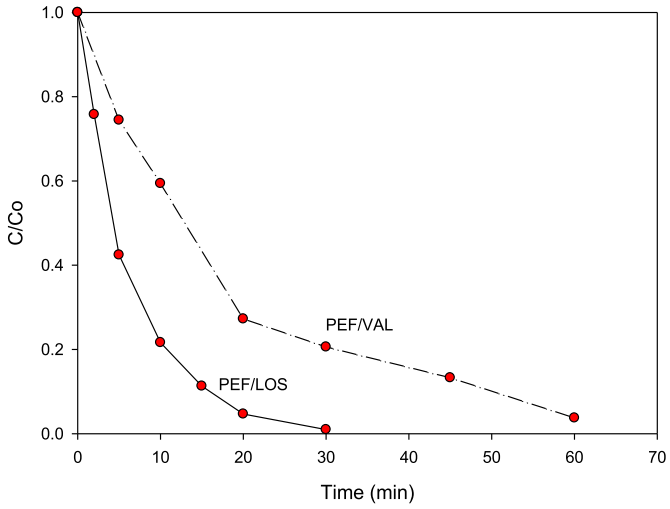

Fig. 1. LOS and VAL degradation by the photo-electro-Fenton (PEF) system. Experimental conditions: [Antihypertensive]: 45 μmol/L, [Na_2SO_4]: 0.05 mol/L, [iron (II)]: 36 μmol/L, $pH_{initial}$: 3.0, *j*: 5.0 mA/cm^2, UVA: 1.4 W/m^2, and V: 200 mL.

(Davis et al., 2014; Salazar et al., 2016). Moreover, in the PEF system, the action of light, and hydroxyl and sulfate radicals in the solution bulk coming from photo-Fenton reactions is very usual (Sirés et al., 2014).

To determine the participation of the routes involving the BDD anode in the pollutants elimination, control experiments of AO were performed (Fig. SM2, in the supporting information). The degradations of VAL and LOS by AO were 13 and 17% after 60 min of treatment, respectively. Additionally, to establish the participation of the direct oxidation of LOS and VAL on the BDD surface (Eq. (4)), cyclic voltammetries (CV) were performed (Fig. SM3). In the case of LOS is evident an oxidation peak at ~1.7 V vs Ag/AgCl (Fig. SM3B), which indicates the transference of electrons from the pollutant to the BDD anode (Eq. (4)). In contrast, the voltammogram for VAL did not show any oxidation peak, suggesting that this antihypertensive has no transference of electrons toward the BDD anode. The above results from the CV also highlight that LOS is more prone to oxidation than VAL.

The results for AO in the Fig. SM2 revealed a low contribution of the anodic routes (Eqs. (1)–(3)) to the pollutants elimination. These degradation routes depend on the diffusion of the pollutant or sulfate electrolyte toward the electrode surface and the applied current density (Sirés and Brillas, 2012). As under tested conditions, the current density is low (which is 5.0 mA/cm^2), the production of radicals or persulfate on the anode (Eqs. (1) and (2)) is also low; this is also supported by the very low accumulation of the electro-generated oxidizing species during the AO test (Fig. SM4).

$$BDD\ (HO\bullet) + LOS/VAL \rightarrow \text{degradation products} \quad (1)$$

$$BDD + 2SO_4^{2-} \rightarrow S_2O_8^{2-} + 2e\text{-} \quad (2)$$

$$S_2O_8^{2-} + LOS/VAL \rightarrow \text{degradation products} \quad (3)$$

$$BDD + LOS/VAL \rightarrow \text{degradation products} + ne\text{-} \quad (4)$$

In the considered configuration for PEF, H_2O_2 is electro-generated from the oxygen reduction in the GDE (Eq. (5)) (as demonstrated by the H_2O_2 accumulation for the BDD/GDE configuration in Fig. SM4) (Sirés et al., 2014). Hydrogen peroxide is an oxidizing agent that could also contribute to the removal of the antihypertensives (Eq. (6)). However, a recent study demonstrated that LOS is hardly degraded by H_2O_2 (at 500 μmol/L) (Guateque-Londoño et al., 2020).

$$GDE + O_2 + 2H^+ + 2e\text{-} \rightarrow H_2O_2 \quad (5)$$

$$H_2O_2 + LOS/VAL \rightarrow \text{degradation products} \quad (6)$$

As above mentioned, in the PEF system, the action of light, and hydroxyl and sulfate radicals (Eqs. (7)–(10)) in the solution bulk coming from photo-Fenton reactions is also plausible. Therefore, the photolysis of the target pharmaceuticals was tested (Fig. SM5). Photolysis of both antihypertensives by the UVA light was discarded because such irradiation showed no significant pollutant elimination even after 60 min of treatment. This can be explained considering that there is no intersection between the lamp emission (which is a peak centered at 368 nm) and the UV spectra of LOS and VAL (which have absorptions at wavelengths <340 nm (Bonfilio et al., 2010; Singh et al., 2011)). The important UVA role is evidenced when the photo-electro-Fenton process is faced with its control system without irradiation (the electro-Fenton treatment (EF)).

LOS degradation by EF and PEF shows that these systems remove 41 and 58% of the pollutant in the first 5 min of treatment, respectively (Data not shown in plots). Likewise, the eliminations of VAL by EF and PEF at 5 min, were 32 and 41%, respectively (Data not shown in plots). The elimination of the antihypertensives is increased in PEF respect to EF thanks to the regeneration of the ferrous ions is accelerated by the UVA light, which subsequently raises the number of radicals (HO• and $SO_4\bullet^-$) available (Eqs. (7)–(10)) to degrade LOS or VAL. Hence, it can be indicated that for the degradation of LOS and VAL, the PEF system presents a strong action of radicals coming from the interaction among iron, H_2O_2 or $S_2O_8^{2-}$ and UVA light (which is supported by the relative low accumulations of oxidants during the treatments of LOS or VAL by PEF, see Fig. SM6), with a minor participation of the anodic oxidation (i.e., direct oxidation for LOS and via adsorbed radicals at the BDD surface for both pollutants).

$$Fe^{2+} + H_2O_2 \rightarrow Fe^{3+} + HO\bullet + HO^- \quad (7)$$

$$Fe^{2+} + S_2O_8^{2-} \rightarrow Fe^{3+} + SO_4\bullet^- + SO_4^{2-} \quad (8)$$

$$HO\bullet, SO_4\bullet^- + LOS/VAL \rightarrow \text{degradation products} \quad (9)$$

$$Fe^{3+} + H_2O + UVA \rightarrow Fe^{2+} + HO\bullet + H^+ \quad (10)$$

It should be mentioned that under the tested conditions, the PEF process has a consumption of electric energy of 5.04 and 16.72 kWh/m^3 to degrade 90% of LOS and VAL, respectively (see Text S1 for the definitions and calculations). A screening of studies, based on the consumption of electric energy per order (E_{EO}) to treat organic pollutants for several AOPs, demonstrated that electrochemical processes as PEF have a moderate E_{EO} (typically ranged between 1 and 100 kWh/m^3, with a median value of 38.1 kWh/m^3). Such E_{EO} values for the electrochemical processes are lower than the reported for UV-based photocatalysis, ultrasound and microwave-based AOPs (which have median values of E_{EO} of 335, 2616 and 543 kWh/m^3, respectively (Miklos et al., 2018)). The above information for pollutants degradation and E_{EO} estimation indicate that PEF process has a high feasibility to treat LOS and VAL in aqueous matrices.

3.2. Effect of the antihypertensive structure - losartan vs. valsartan

LOS and VAL belong to sartan-type antihypertensives, which comprises several compounds sharing a common nucleus. Indeed, LOS was the first antihypertensives-type, and the synthesis of the other sartan pharmaceuticals was based on its structure (Nödler et al., 2013). The pharmaceuticals LOS and VAL contain a biphenyl-tetrazole nucleus; LOS additionally has chlorine, butyl, and methoxyl groups bonded to an imidazole ring, whereas VAL exhibits a carboxylic acid linked to a pentanamide moiety (Fig. 2).

As observed from Fig. 1, LOS exhibited a faster degradation than VAL in the PEF system. To better understand the differences, kinetics and structural aspects were considered. The degradations of VAL and LOS by PEF adjusted well to pseudo-first-order kinetics (i.e., the plots of Ln (C/Co) vs. time of these antihypertensives have a linear form, Fig. SM7). The corresponding degradation rate constants (k) for LOS and VAL were 0.154 and 0.054 min^{-1}, respectively. The unlike k values could be related to differences in LOS and VAL interaction with the degrading agents.

The degrading species involved in the PEF process (i.e., persulfate anion or radicals, even the anode) typically attack the regions rich in electron density on the pollutants (Serna-Galvis et al., 2017). Hence, theoretical analyses of atomic charge (AC) for LOS and VAL were performed (Tables SM1-SM2) to provide a rough idea of electron density on the antihypertensives (Ionescu et al., 2015)). A

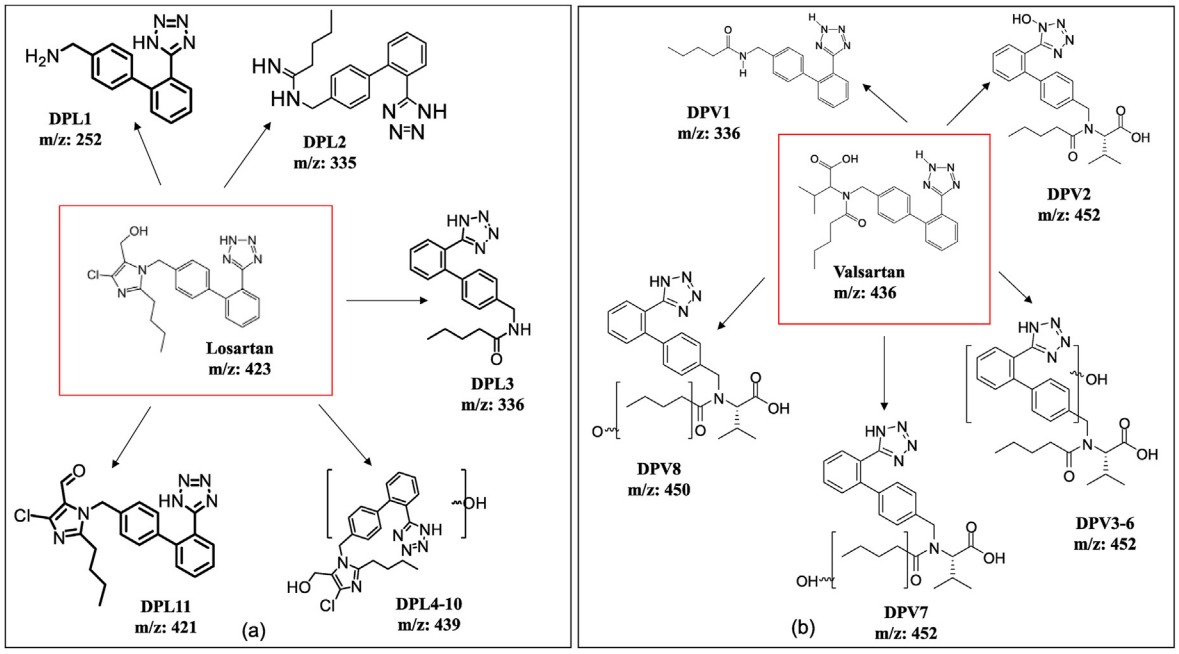

Fig. 2. Primary degradation products generated by photo-electro-Fenton treatment using BDD anodes for (a) losartan and (b) valsartan.

more negative value of AC indicates a higher electron density. From Tables SM1-SM2, it can be noted that the antihypertensives have different atomic charge distributions, even in the common nucleus that they differ. In fact, the addition of charges corresponding to tetrazole moiety is more negative for LOS than for VAL. Furthermore, the charges summation of all substituents attached at the common nucleus for LOS ($\Sigma = -0.040$ -0.359 -0.068 + 0.391 = −0.076) is more negative than for VAL ($\Sigma = -0.420 + 0.620 - 0.213 = -0.013$), which suggests that globally the substituents on LOS have more electron density than those on VAL. Consequently, LOS exhibits a higher reactivity toward the degrading species (i.e., this antihypertensive is easier to oxidize), which explains its faster degradation (and a higher k value) by the PEF system (Fig. SM7). The precedent theoretical calculations correlate well with the results of the CV analysis for both compounds, which also show that LOS can be easier oxidized than VAL on the BDD surface. In fact, for VAL no direct oxidation is observed (Fig. SM3 B and C), whereas LOS evidenced a clear oxidative signal in the cyclic voltammogram at ~1.7 V vs. Ag/AgCl.

3.3. *Primary transformations of the antihypertensives and mineralization by PEF action*

To deeply study the PEF action on the target pollutants, the initial transformations were established through UHPLC-HRMS analyses. Fig. 2A presents the chemical structure of the primary degradation products of losartan (DPL). Three products coming from imidazole ring rupture (DPL1, DPL2, and DPL3), several isomers of hydroxylation of the biphenyl-tetrazole moiety (DPL4-10) and one product of alcohol group oxidation (DPL11) were found. In the case of VAL, products generated after decarboxylation (DPV1), hydroxylations of tetrazole (DPV2), biphenyl (generating three isomers, DPL3-6) and amide (DPV7), in addition to oxidation (DPV8) the linear-alkyl group on the pentanamide moiety were identified (Fig. 2B). More information about these TPs can be found in a recent paper (Serna-Galvis et al., 2019b), where these two antihypertensives were subjected to sonochemical degradation.

In addition to the structural elucidation, the normalized evolution of the products was established (Fig. SM8). It can be observed that DPL1, DPL2, DPL3, and DPL11 are faster formed than the other products. This indicates that imidazole and alcohol on LOS are the most reactive sites to the degrading agents. Indeed, radical species (as HO•) interacts fastly with heterocyclic rings as imidazole (Llano and Eriksson, 1999), because such functional groups have a high electron availability (as indicated by the theoretical analyses of atomic charges presented in Table SM1). The successive attacks of radical species can promote the imidazole ring-opening (Cheng et al., 2010), as observed from the structure of DPL1, DPL2, and DPL3.

Furthermore, it can be mentioned that alcohols are also prone to oxidation by radicals through hydrogen abstraction to produce the respective aldehyde. Indeed, alcohols are typically used as scavengers due to their high reactivity towards hydroxyl or sulfate radicals (Billany et al., 1996; He et al., 2014). This explains the favorable attack by the radicals to the alcohol group on LOS to generate DPL11.

The high number of isomers by attacks to the biphenyl-tetrazole nucleus (DPL 4–10) suggests that such a portion of LOS is also very reactive towards electron-deficient degrading species. It is recognized that HO• and $SO_4^{\bullet-}$ can react with double bonds on the benzene rings (which also concentrate electron density, as reflected by the negative charges on carbons of the biphenyl moiety in Table SM1), to produce hydroxylated substances (He et al., 2014; Khan et al., 2017; Liu et al., 2016). In turn, the tetrazole group (another electron-rich region on LOS, see Table SM1) is also susceptible to hydroxylation by the action of the radicals. It has been proposed that the successive attacks of radical species to such moiety can also cleavage this ring (Gurkan et al., 2012).

Regarding transformation products from VAL, it can be noted that DPV1 and DPV2 are firstly formed (Fig. 2B), indicating the high reactivity of tetrazole and carboxylic acid moieties on the antihypertensive. This was also coincident with the most negative values obtained for these moieties from the atomic charge analyses for VAL (Table SM2). As previously mentioned, the tetrazole group can experiment hydroxylations by the radicals' action, and it is well-known that HO• and $SO_4^{\bullet-}$ can promote decarboxylations of

organic molecules (Steffen et al., 1991; Yang et al., 2015). Similar to LOS, some isomers from hydroxylations to the biphenyl group are formed (Fig. 2A), due to this molecular region on VAL has a considerable electron density (see the negative charges on carbons of such moiety in Table SM2). Additionally, it can be noted that the pentanamide group of VAL also concentrates electron density, which makes this part of the pollutant very available for attacks of the electron-deficient degrading species, leading to DPV7 and DPV8 formation.

Interestingly, the degradations of LOS by other electrochemical, sonochemical and photochemical (based on UVC) processes have also reported products formed through attacks of the radical species to biphenyl-tetrazole rings, imidazole and alcohol moieties (Kaur and Dulova 2020; Martínez-Pachón et al., 2018, 2019; Salazar et al., 2016; Serna-Galvis et al., 2019b). Likewise, in VAL, strong modifications to the carboxylic and amide groups have also been found by other electrochemical systems (Martínez-Pachón et al., 2019). Moreover, during the sonochemical treatment of antihypertensive, same DPV2, DVP7, and DPV8 were obtained (Serna-Galvis et al., 2019b) than in our treatment by PEF. The similarities between the degradation products obtained by PEF and those reported for other processes in the literature suggest identical elimination routes, which is logical, considering that the main degrading role is exerted by the radicals such as HO• and SO_4•$^-$.

It is important to remark that the primary transformations induced by the PEF process and reported in the literature agree well with the reactive sites on LOS and VAL indicated by the theoretical analyses presented in the previous section (Tables SM1-SM2). This reveals the high utility of atomic charge analyses as a qualitative-predictive tool for understanding the initial transformations induced by processes as PEF.

After understanding the primary transformations of both LOS and VAL by PEF, the mineralization of these pollutants was tested. Fig. 3 shows the TOC evolution. As seen, the TOC decreasing is fast until the first 60 min of treatment, reaching ~18% of mineralization. Nevertheless, TOC elimination is slowly increased to 33−38%% after 5 h of electrolysis. This suggests that the compounds coming from the successive attacks of radicals to the primary products of LOS or VAL are more recalcitrant to the action of the PEF process (Martínez-Pachón et al., 2018).

As evidenced by the chemical structures of the primary products (Fig. 2), the PEF process's first transformations lead to oxidations, hydroxylations, fragmentations (even decarboxylation) of the parent pollutants. It is well-known that the subsequent steps (i.e., the successive attacks of radicals to the primary intermediates of LOS or VAL) generate short-chain molecules (e.g., aliphatic acids). Such short-chain acids are recalcitrant to the action of radicals as HO• and trend to accumulate in the solution (Antonin et al., 2015; Skoumal et al., 2009), as also reported for treatment of VAL by PEF using DSA anodes (which exhibited the accumulation of succinic and malic acids after 5 h of the electrochemical process application) (Martínez-Pachón et al., 2018). It can be mentioned that highly oxidized, and short-chain molecules (e.g., aliphatic acids) are biocompatible (Feng et al., 2019; Martínez-Pachón et al., 2018). Then, it can be suggested that this electrochemical system may transform both LOS and VAL into products more friendly for the environment.

3.4. Matrix effect on the LOS degradation by PEF

In the previous sections, it has been considered the degradation of the antihypertensives in the simplest matrix (distilled water) and at the ideal pH for the Fenton-based processes (i.e., pH ~ 3.0 (Antonin et al., 2015; Pignatello et al., 2006)). However, the actual applications of the PEF process demand the operation at higher pH values and in aqueous matrices more complex than distilled water. Therefore, the degradation of LOS (which was selected because the fastest degradation in the simplest matrix, Fig. 1) by PEF at a higher pH value (which was 5.0) was tested. Also, the degradation of LOS in the presence of oxalic acid (a compound widely used at the pharmaceutical manufacture (Transparency Market Research, 2020), which can be present in wastewaters of such industries) was assessed. Additionally, the treatment by PEF of a real effluent of municipal wastewater treatment plant doped with LOS was performed.

In Fig. 4A, the removal of LOS by PEF at pH 5.0 is presented. It can be noted that at pH 5.0, the degradation was slower than at pH 3.0. Nonetheless, the PEF process at the higher pH degraded completely the antihypertensive after 90 min of treatment. The differences between pH 3.0 and 5.0 can be associated with the aqueous

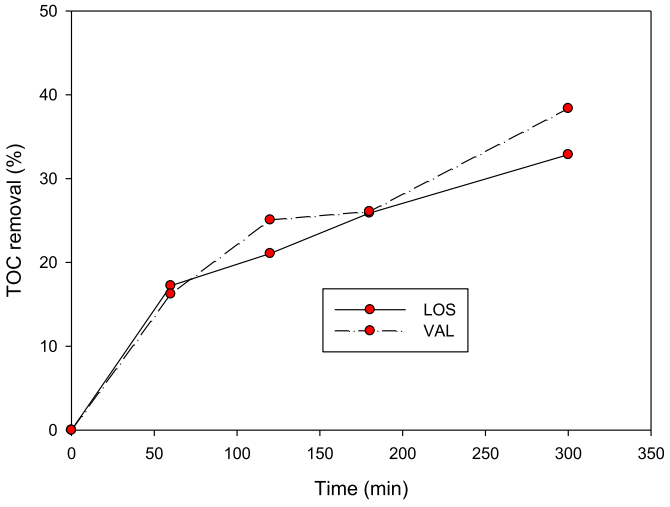

Fig. 3. TOC evolution during the treatment of LOS and VAL by PEF. Experimental conditions: [Antihypertensive]: 45 μmol/L, [Na_2SO_4]: 0.05 mol/L, [iron (II)]: 36 μmol/L, $pH_{initial}$: 3.0, *j*: 5.0 mA/cm^2, UVA: 1.4 W/m^2, and V: 200 mL. $TOC_{initial}$: 12.1 mg C/L.

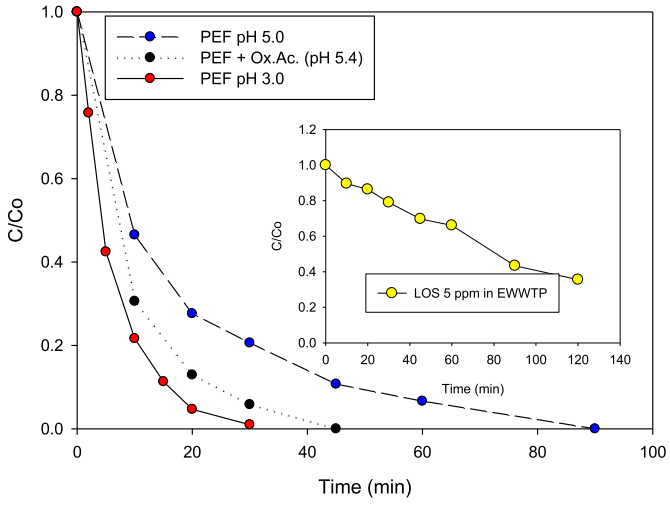

Fig. 4. Degradation of LOS in the presence of oxalic acid by PEF (BDD/GDE/UVA/Na_2SO_4) at pH 3.0 and pH ~5.0 in absence of oxalic acid, plus at pH 5.0 in presence of oxalic acid (Ox. Ac, 40 μmol/L). Experimental conditions: [LOS]: 45 μmol/L, V: 200 mL, [Fe^{2+}]: 36 μmol/L, [Oxalic acid]: 40 μmol/L, [Na_2SO_4]: 0.05 mol/L, *j*: 5.0 mA/cm^2, and UVA: 1.4 W/m^2. **Inset.** LOS (5 mg/L: 11.25 μmol/L) degradation in real complex water (EWWTP).

chemistry of iron, mainly the speciation of Fe (III). At pH 5.0, the first step of Fenton reaction involves a species (i.e., $[Fe(H_2O)_4(OH)_2]$, Eq. (11)) ~10 times more reactive than Fe^{2+} (which predominates at pH 3.0, Eqs. (7)–(10)) toward hydrogen peroxide. However, at pH 5.0, a portion of the Fe (III) ions experiments precipitation as amorphous ferric oxyhydroxides (Eq. (12)). These oxyhydroxides are little photo-active, and due to their colloidal nature, they may scatter the light (Pignatello et al., 2006), limiting the production of radicals through Eq. (10). Consequently, the LOS degradation at pH 5.0 is lower than at pH 3.0.

$$[Fe(H_2O)_4(OH)_2] + H_2O_2 \rightarrow [Fe(H_2O)_4(OH)_2]^+ + HO\bullet + HO^- \quad (11)$$

$$[Fe(H_2O)_4(OH)_2]^+ + HO^- \rightarrow \rightarrow \rightarrow \text{other polynuclear species} \quad (12)$$

Interestingly, in the presence of oxalic acid at pH 5.4, the LOS removal was improved with respect to degradation at pH 5.0, achieving 100% of pollutant elimination after 45 min of the process application (Fig. 4A). The oxalic acid is a well-known complexing agent of Fe (III) (Eq. (13)), and its presence in the aqueous media avoids the precipitation of iron as ferric oxyhydroxides (Martínez-Pachón et al., 2018; Pignatello et al., 2006). The ferric-oxalic acid complexes are soluble forms susceptible to photo-decomposition by UVA light action through a ligand to metal charge transfer mechanism (Martínez-Pachón et al., 2018; Pignatello et al., 2006), leading to the regeneration of Fe (II) and yielding oxalate radicals (Eq. (14)). Oxalate radical can combine with the dissolved oxygen to form anion radical superoxide (Eq. (15)), which can evolve until hydrogen peroxide (Eq. (16)). This provides another source of hydrogen peroxide for the Fenton reaction (Eq. (7)) to generate more hydroxyl radicals. Moreover, oxalate radicals can decompose itself into CO_2 and $CO_2\bullet^-$ (Eq. (17)). This last species has a high redox potential (E° ~ 1.9 V) (Kwan and Chu, 2007; Prato-Garcia et al., 2009), which could act as a degrading agent of LOS. All these aspects explain the positive effect of the presence of oxalic acid at pH 5.4. Hence, the results suggest that PEF can effectively treat pharmaceutical wastewater, having mixtures of oxalic acid and LOS.

$$Fe^{3+} + 3C_2O_4^{2-} \rightarrow [Fe(C_2O_4)_3]^{3-} \quad (13)$$

$$[Fe(C_2O_4)_3]^{3-} + UVA \rightarrow Fe^{2+} + 2C_2O_4^{2-} + 2C_2O_4\bullet^- \quad (14)$$

$$C_2O_4\bullet^- + O_2 \rightarrow 2CO_2 + O_2\bullet^- \quad (15)$$

$$O_2\bullet^- + 2H^+ + Fe^{2+} \rightarrow H_2O_2 + Fe^{3+} \quad (16)$$

$$C_2O_4\bullet^- \rightarrow CO_2 + CO_2\bullet^- \quad (17)$$

On the other hand, the effluent of municipal wastewater plant from Bogotá-Colombia (EWWTP, Table SM3) doped with LOS (at 11.25 μmol/L, an amount lower than previously used, this to obtain a better approximation to actual concentrations in wastewater) was treated by PEF (Fig. 4B). It was found that the process led to a high degradation of LOS (64% after 120 min of treatment) in such complex matrix. Although the process was able to remove the antihypertensive in the EWWTP, its degradation was slower than in distilled water (even when the initial concentration of LOS was lower). This EWWTP includes a pre-treatment based on the partial removal of suspended solids with a screening unit to filter large objects that may cause difficulties of operation in the subsequent processes. Also, includes a primary treatment based on the partial removal of organic matter through coagulation, flocculation and sedimentation, likewise fat and grease is also removed in this treatment, with a removal efficiency of 40% BOD and 60% of suspended solids, as well as with an average flow rate of wastewater treated over 1 year the 4 m^3/s (ca. 350,000 m^3/day) to be disposed of in the Bogotá river. A revision of the EWWTP composition shows that this water has a considerable content of other organic matter (see its COD and TOC values) and ionic substances (as indicated by alkalinity and conductivity) that compete with LOS by the degrading agents as radicals (Salazar et al., 2016). Also, the turbidity and solids in the sample can affect the light action. Moreover, the pH of EWWTP was near neutral (7.65), which decreases the availability of photo-active iron forms as above explained (Eq. (15)). Hence, these matrix aspects eliminate the pollutant in the complex matrix slower than in the distilled water.

4. Conclusions

The treatment of sartan-type antihypertensives by PEF (at mild conditions of current, light, and iron concentration) effectively degraded them in both distilled water and effluent of the wastewater treatment plant. Due to the action of oxidizing species (as hydroxyl radical and sulfate radical), in addition to anodic route, the PEF process was able to degrade both LOS and VAL. The structural differences between LOS and VAL determined their interaction with the degrading agents generated in PEF. Indeed, LOS exhibits a higher reactivity toward the species, such as HO•, which is justified by both the faster degradation (a higher k value) and higher atomic charges than VAL. Besides, the generated radicals reacted with the biphenyl-tetrazole rings, imidazole, and alcohol moieties on LOS. Meanwhile, VAL experimented modification on the carboxyl and pentanamide moieties, plus hydroxylations on its biphenyl-tetrazole nucleus. Such modifications on both pollutants agreed well with the reactive sites indicated by the theoretical calculations, revealing the high utility of atomic charge analyses for rationalizing the primary transformations induced by PEF. This electrochemical process-induced partial mineralization of the two target pollutants (between 33 and 38% after 5 h of treatment) indicates that the compounds coming from the primary products are more recalcitrant to the action of PEF. Additionally, the treatment of LOS at pH around 5 was improved by the presence of oxalic acid. Thanks to this compound, the precipitation of iron (III) as ferric oxyhydroxides is avoided, and the photo-regeneration of iron (II) and production of extra radicals are favored. Finally, the process led to a high degradation of LOS in the municipal wastewater treatment plant; however, such degradation was slower than in distilled water because of the interfering effects of the matrix components. The good results about degradation in the effluent and oxalic acid's presence indicate the high potentiality of PEF application to degrade sartan-type antihypertensives in complex matrices containing both organic and inorganic matter.

Credit author statement

Diana Martínez-Pachón: Investigation, Methodology; Formal analysis, Writing-original draft. **Efraím A. Serna-Galvis**: Conceptualization, Formal analysis, Writing-original draft, Writing-review & editing. **María Ibañez**: Methodology; Writing-review & editing. **Félix Hernández**: Methodology; Writing-review & editing. **Yenny Ávila-Torres**: Software, Formal analysis. **Ricardo A. Torres-Palma**: Conceptualization, Writing-review & editing, Resources, Funding acquisition. **Alejandro Moncayo-Lasso**: Conceptualization, Writing-review & editing, Resources, Funding acquisition.

Declaration of competing interest

The authors declare that they have no known competing

financial interests or personal relationships that could have appeared to influence the work reported in this paper.

Acknowledgments

The authors from Universidad Antonio Nariño thank MINCIENCIAS COLOMBIA (before known as COLCIENCIAS) for funding through project No. 123384467057 (contract 818–2019 - Call 844–2019). The authors from GIRAB thank Universidad de Antioquia UdeA for the support provided to their research group through "Programa de Sostenibilidad" and the financing from MINCIENCIAS COLOMBIA (before named COLCIENCIAS) through the project No. 111577757323 (Convocatoria 777 de 2017). Authors from IUPA (UJI) acknowledge the financial support of Ministerio de Ciencia, Innovación y Universidades, Spain (Ref RTI 2018-097417-B-I00) and Generalitat Valenciana (Research Group of Excellence, Prometeo 2019/040). E.A. Serna-Galvis thanks the doctoral scholarship provided by MINCIENCIAS COLOMBIA (before named COLCIENCIAS) from July 2015 to June 2019 through Convocatoria 647 de 2014. Y. Ávila-Torres thanks Universidad Santiago de Cali for the support provided through the project DGI 939-621120-1867.

Appendix A. Supplementary data

Supplementary data to this article can be found online at https://doi.org/10.1016/j.chemosphere.2020.129491.

References

Antonin, V.S., Santos, M.C., Garcia-Segura, S., Brillas, E., 2015. Electrochemical incineration of the antibiotic ciprofloxacin in sulfate medium and synthetic urine matrix. Water Res. 83, 31–41. https://doi.org/10.1016/j.watres.2015.05.066.

Bayer, A., Asner, R., Schüssler, W., Kopf, W., Weiß, K., Sengl, M., Letzel, M., 2014. Behavior of sartans (antihypertensive drugs) in wastewater treatment plants, their occurrence and risk for the aquatic environment. Environ. Sci. Pollut. Res. 21, 10830–10839. https://doi.org/10.1007/s11356-014-3060-z.

Berkner, S., Thierbach, C., 2014. Biodegradability and transformation of human pharmaceutical active ingredients in environmentally relevant test systems. Environ. Sci. Pollut. Res. 21, 9461–9467. https://doi.org/10.1007/s11356-013-1868-6.

Billany, M.R., Khatib, K., Gordon, M., Sugden, J.K., 1996. Alcohols and ethanolamines as hydroxyl radical scavengers. Int. J. Pharm. 137, 143–147. https://doi.org/10.1016/0378-5173(96)04246-9.

Bonfilio, R., Favoretto, L.B., Pereira, G.R., Azevedo, R.D.C.P., Araújo, M.B. de, 2010. Comparative study of analytical methods by direct and first-derivative UV spectrophotometry for evaluation of losartan potassium in capsules. Brazilian J. Pharm. Sci. 46, 147–155. https://doi.org/10.1590/S1984-82502010000100017.

Botero-Coy, A.M., Martínez-Pachón, D., Boix, C., Rincón, R.J., Castillo, N., Arias-Marín, L.P., Manrique-Losada, L., Torres-Palma, R.A., Moncayo-Lasso, A., Hernández, F., 2018. An investigation into the occurrence and removal of pharmaceuticals in Colombian wastewater. Sci. Total Environ. 642, 842–853. https://doi.org/10.1016/j.scitotenv.2018.06.088.

Cheng, Q., Gu, J., Compaan, K.R., Schaefer, H.F., 2010. Hydroxyl radical reactions with adenine: reactant complexes, transition states, and product complexes. Chem. Eur J. 16, 11848–11858. https://doi.org/10.1002/chem.201001236.

ClinClac, 2018. Valsartan-number of prescriptions over time (2007-2017) [WWW Document]. Clincalc.com. https://clincalc.com/DrugStats/Drugs/Valsartan.

Dao, K.C., Yang, C.-C., Chen, K.-F., Tsai, Y.-P., 2020. Recent trends in removal pharmaceuticals and personal care products by electrochemical oxidation and combined systems. Water 12, 1043. https://doi.org/10.3390/w12041043.

Davis, J., Baygents, J.C., Farrell, J., 2014. Understanding persulfate production at boron doped diamond film anodes. Electrochim. Acta 150, 68–74. https://doi.org/10.1016/j.electacta.2014.10.104.

Feng, L., Serna-Galvis, E.A., Oturan, N., Giannakis, S., Torres-Palma, R.A., Oturan, M.A., 2019. Evaluation of process influencing factors, degradation products, toxicity evolution and matrix-related effects during electro-Fenton removal of piroxicam from waters. J. Environ. Chem. Eng. 7, 103400 https://doi.org/10.1016/j.jece.2019.103400.

Godoy, A.A., Kummrow, F., Pamplin, P.A.Z., 2015. Ecotoxicological evaluation of propranolol hydrochloride and losartan potassium to Lemna minor L. (1753) individually and in binary mixtures. Ecotoxicology 24, 1112–1123. https://doi.org/10.1007/s10646-015-1455-3.

Guateque-Londoño, J.F., Serna-Galvis, E.A., Ávila-Torres, Y., Torres-Palma, R.A., 2020. Degradation of losartan in fresh urine by sonochemical and photochemical advanced oxidation processes. Water 12, 3398. https://doi.org/10.3390/w12123398.

Gurkan, Y.Y., Turkten, N., Hatipoglu, A., Cinar, Z., 2012. Photocatalytic degradation of cefazolin over N-doped TiO2 under UV and sunlight irradiation: prediction of the reaction paths via conceptual DFT. Chem. Eng. J. 184, 113–124. https://doi.org/10.1016/j.cej.2012.01.011.

Gurke, R., Rößler, M., Marx, C., Diamond, S., Schubert, S., Oertel, R., Fauler, J., 2015. Science of the Total Environment Occurrence and removal of frequently prescribed pharmaceuticals and corresponding metabolites in wastewater of a sewage treatment plant. Sci. Total Environ. 532, 762–770. https://doi.org/10.1016/j.scitotenv.2015.06.067.

He, X., Mezyk, S.P., Michael, I., Fatta-Kassinos, D., Dionysiou, D.D., 2014. Degradation kinetics and mechanism of β-lactam antibiotics by the activation of H2O2 and Na2S2O8 under UV-254nm irradiation. J. Hazard Mater. 279, 375–383. https://doi.org/10.1016/j.jhazmat.2014.07.008.

Ionescu, C.M., Sehnal, D., Falginella, F.L., Pant, P., Pravda, L., Bouchal, T., Svobodová Vařeková, R., Geidl, S., Koča, J., 2015. AtomicChargeCalculator: interactive web-based calculation of atomic charges in large biomolecular complexes and drug-like molecules. J. Cheminf. 7, 1–13. https://doi.org/10.1186/s13321-015-0099-x.

Israili, Z.H., 2000. Clinical pharmacokinetics of angiotensin II (AT 1) receptor blockers in hypertension. J Hum Hypertens Suppl 1, S73–S87.

Kaur, B., Dulova, N., 2020. UV-assisted chemical oxidation of antihypertensive losartan in water. J. Environ. Manag. 261, 110170. https://doi.org/10.1016/j.jenvman.2020.110170.

Khan, S., He, X., Khan, J.A., Khan, H.M., Boccelli, D.L., Dionysiou, D.D., 2017. Kinetics and mechanism of sulfate radical- and hydroxyl radical-induced degradation of highly chlorinated pesticide lindane in UV/peroxymonosulfate system. Chem. Eng. J. 318, 135–142. https://doi.org/10.1016/j.cej.2016.05.150.

Kwan, C.Y., Chu, W., 2007. The role of organic ligands in ferrous-induced photochemical degradation of 2,4-dichlorophenoxyacetic acid. Chemosphere 67, 1601–1611. https://doi:10.1016/j.chemosphere.2006.11.052.

Liu, Y., He, X., Fu, Y., Dionysiou, D.D., 2016. Kinetics and mechanism investigation on the destruction of oxytetracycline by UV-254 nm activation of persulfate. J. Hazard Mater. 305, 229–239. https://doi.org/10.1016/j.jhazmat.2015.11.043.

Llano, J., Eriksson, L.A., 1999. Mechanism of hydroxyl radical addition to imidazole and subsequent water elimination. J. Phys. Chem. 103, 5598. https://doi.org/10.1021/jp9902957.

Martínez-Pachón, D., Ibáñez, M., Hernández, F., Torres-Palma, R.A., Moncayo-Lasso, A., 2018. Photo-electro-Fenton process applied to the degradation of valsartan: effect of parameters, identification of degradation routes and mineralization in combination with a biological system. J. Environ. Chem. Eng. 6, 7302–7311. https://doi.org/10.1016/j.jece.2018.11.015.

Martínez-Pachón, D., Espinosa-Barrera, P., Rincón-Ortíz, J., Moncayo-Lasso, A., 2019. Advanced oxidation of antihypertensives losartan and valsartan by photo-electro-Fenton at near-neutral pH using natural organic acids and a dimensional stable anode-gas diffusion electrode (DSA-GDE) system under light emission diode (LED) lighting. Environ. Sci. Pollut. Res. 26, 4426–4437. https://doi.org/10.1007/s11356-018-2645-3.

Miklos, D.B., Remy, C., Jekel, M., Linden, K.G., Hübner, U., 2018. Evaluation of advanced oxidation processes for water and wastewater treatment- A critical review. Water Res. 139, 118–131. https://doi.org/10.1016/j.watres.2018.03.042.

Mikulic, M., 2020. Number of losartan potassium prescriptions in the U.S. from 2004 to 2017 [WWW Document]. Stat. GmbH. https://www.statista.com/statistics/781681/losartan-potassium-prescriptions-number-in-the-us/.

Moreira, F.C.F.C., Boaventura, R.A.R.R., Brillas, E., Vilar, V.J.P.P., 2017. Electrochemical advanced oxidation processes: a review on their application to synthetic and real wastewaters. Appl. Catal. B Environ. 202, 217–261. https://doi.org/10.1016/j.apcatb.2016.08.037.

Nödler, K., Hillebrand, O., Idzik, K., Strathmann, M., Schiperski, F., Zirlewagen, J., Licha, T., 2013. Occurrence and fate of the angiotensin II receptor antagonist transformation product valsartan acid in the water cycle - a comparative study with selected β-blockers and the persistent anthropogenic wastewater indicators carbamazepine and acesulfame. Water Res. 47, 6650–6659. https://doi.org/10.1016/j.watres.2013.08.034.

Olvera-Vargas, H., Gore-Datar, N., Garcia-Rodriguez, O., Mutnuri, S., Lefebvre, O., 2021. Electro-Fenton treatment of real pharmaceutical wastewater paired with a BDD anode: reaction mechanisms and respective contribution of homogeneous and heterogeneous OH. Chem. Eng. J. 404, 126524 https://doi.org/10.1016/j.cej.2020.126524.

Pignatello, J.J., Oliveros, E., Mackay, A., 2006. Advanced oxidation processes for organic contaminant destruction based on the Fenton reaction and related chemistry. Crit. Rev. Environ. Sci. Technol. 36, 1–84. https://doi.org/10.1080/10643380500326564.

Prato-Garcia, D., Vasquez-Medrano, R., Hernandez-Esparza, M., 2009. Solar photo-assisted advanced oxidation of synthetic phenolic wastewaters using ferrioxalate complexes. Sol. Energy 83, 306–315. https://doi:10.1016/j.solener.2008.08.005.

Roveri, V., Guimarães, L.L., Toma, W., Correia, A.T., 2020. Occurrence and ecological risk assessment of pharmaceuticals and cocaine in a beach area of Guarujá, São Paulo State, Brazil, under the influence of urban surface runoff. Environ. Sci. Pollut. Res. 27, 45063–45075. https://doi.org/10.1007/s11356-020-10316-y.

Salazar, C., Contreras, N., Mansilla, H.D., Yáñez, J., Salazar, R., 2016. Electrochemical degradation of the antihypertensive losartan in aqueous medium by electro-oxidation with boron-doped diamond electrode. J. Hazard Mater. 319, 84–92. https://doi.org/10.1016/j.jhazmat.2016.04.009.

Sehnal, D., 2020. AtomicChargeCalculator [WWW document]. WebChemistry. https://webchem.ncbr.muni.cz/Platform/ChargeCalculator.

Serna-Galvis, E.A., Silva-Agredo, J., Giraldo-Aguirre, A.L., Torres-Palma, R.A., 2015. Sonochemical degradation of the pharmaceutical fluoxetine: effect of parameters, organic and inorganic additives and combination with a biological system. Sci. Total Environ. 524–525, 354–360. https://doi.org/10.1016/j.scitotenv.2015.04.053.

Serna-Galvis, E.A., Ferraro, F., Silva-Agredo, J., Torres-Palma, R.A., 2017. Degradation of highly consumed fluoroquinolones, penicillins and cephalosporins in distilled water and simulated hospital wastewater by UV254 and UV254/persulfate processes. Water Res. 122, 128–138. https://doi.org/10.1016/j.watres.2017.05.065.

Serna-Galvis, E.A., Silva-Agredo, J., Botero-Coy, A.M., Moncayo-Lasso, A., Hernández, F., Torres-Palma, R.A., 2019a. Effective elimination of fifteen relevant pharmaceuticals in hospital wastewater from Colombia by combination of a biological system with a sonochemical process. Sci. Total Environ. 670, 623–632. https://doi.org/10.1016/j.scitotenv.2019.03.153.

Serna-Galvis, E.A., Isaza-Pineda, L., Moncayo-Lasso, A., Hernández, F., Ibáñez, M., Torres-Palma, R.A., 2019b. Comparative degradation of two highly consumed antihypertensives in water by sonochemical process. Determination of the reaction zone, primary degradation products and theoretical calculations on the oxidative process. Ultrason. Sonochem. 58, 104635 https://doi.org/10.1016/j.ultsonch.2019.104635.

Singh, S., Yadav, A.K., Gautam, H., 2011. Simultaneous estimation of valsartan and hydrochlorothiazide in tablets by rp-hplc method. Bull. Pharmaceut. Res. 170–174.

Sirés, I., Brillas, E., 2012. Remediation of water pollution caused by pharmaceutical residues based on electrochemical separation and degradation technologies : a review. Environ. Int. 40, 212–229. https://doi.org/10.1016/j.envint.2011.07.012.

Sirés, I., Brillas, E., Oturan, M.A., Rodrigo, M.A., Panizza, M., 2014. Electrochemical advanced oxidation processes: today and tomorrow. A review. Environ. Sci. Pollut. Res. 21, 8336–8367. https://doi.org/10.1007/s11356-014-2783-1.

Skoumal, M., Rodríguez, R.M., Cabot, P.L., Centellas, F., Garrido, J.A., Arias, C., Brillas, E., 2009. Electro-Fenton, UVA photoelectro-Fenton and solar photoelectro-Fenton degradation of the drug ibuprofen in acid aqueous medium using platinum and boron-doped diamond anodes. Electrochim. Acta 54, 2077–2085. https://doi.org/10.1016/j.electacta.2008.07.014.

Steffen, L.K., Glass, R.S., Sabahi, M., Wilson, G.S., Schoeneich, C., Mahling, S., Asmus, K.D., 1991. Hydroxyl radical induced decarboxylation of amino acids. Decarboxylation vs bond formation in radical intermediates. J. Am. Chem. Soc. 113, 2141–2145. https://doi.org/10.1021/ja00006a035.

Transparency Market Research, 2020. Oxalic acid Market [WWW document]. Oxalic acid mark. - glob. Ind. Anal. Size, share, growth, trends, forecast 2019 - 2027. https://www.transparencymarketresearch.com/oxalic-acid-market.html.

Yang, Y., Jiang, J., Lu, X., Ma, J., Liu, Y., 2015. Production of sulfate radical and hydroxyl radical by reaction of ozone with peroxymonosulfate: a novel advanced oxidation process. Environ. Sci. Technol. 49, 7330–7339. https://doi.org/10.1021/es506362e.